# Flow - Induced Dilation of Cohesive Granular Materials

**AbdulMobeen Faqih, Bodhisattwa Chaudhuri, Fernando J. Muzzio, and M. Silvina Tomassone**
Dept. of Chemical and Biochemical Engineering, Rutgers University, Piscataway, NJ 08854

**Albert Alexander**
Astrazeneca Pharmaceuticals LP, 1800 Concord Pike, Wilmington, DE 19850

**Steve Hammond**
Pfizer, Inc., 100 Route 206 N, Peapack, NJ 07977

*DOI 10.1002/aic.11014*
*Published online November 3, 2006 in Wiley InterScience (www.interscience.wiley.com).*

*Dynamic (flow — induced) expansion (dilation) of fine powders inside a rotating drum is investigated. Most previous work on powder dilation is based on two-phase effects, where the presence of air either drives the flow (fluidized bed), or air needs to be displaced for the powder to flow (hoppers). Experimental results show that for many common powders the bed dilates visibly up to 25%, depending on powder composition, particle size, and the rotation speed of the drum. Discrete element simulations were performed in parallel for various values of powder cohesion, rotation rates, and drum size. Results show qualitative agreement between experiments and simulations. In experiments, after the initial transient behavior, the density reached at equilibrium for all materials tested is lower than the static "bulk density" reported in the literature. In both experiments and simulations, increase in powder cohesion enhances dilation. DEM simulations are used to analyze local density fluctuations and coordination numbers, which decrease with increasing cohesion. As cohesive forces become dominant, large pores are formed in the bed, leading to substantial fluctuations in local (micro) density that can have tremendous consequences for product uniformity and quality.* © 2006 American Institute of Chemical Engineers *AIChE J,* 52: 4124–4132, 2006
*Keywords: dilation, granular flow, discrete element method*

## Introduction

Storage and flow of cohesive powders is relevant to many industries including food, agriculture, mining, and pharmaceuticals. Since the pioneering work of Bagnold,[1,2] extensive work has focused on the area of particle flow properties of noncohesive materials.[3-5] To this date, the majority of research has been carried out for cohesionless materials, [6-9] with particle size larger than 100 $\mu$m. Fundamental studies of fine powders (particle diameter between $\sim$ 1 $\mu$m and $\sim$ 100 $\mu$m) have been scarce despite their commercial importance.

Some recent studies have added water or oil to glass beads or sand to "simulate" cohesion,[9-13] but dry fine particles where cohesion is due to forces other than capillary surface tension effects have only recently been taken into consideration in the past few years.[14-17] For these materials, as the particle-size decreases, the interparticle forces (for example, van der Waals forces) become stronger leading to an increase in cohesion. The increase in cohesion plays a dominant role in flow dynamics as it directly impacts the bulk flowability of solid material. In-

Correspondence concerning this article should be addressed to M. S. Tomassone at silvana@soemail.rutgers.edu.

creased cohesiveness can cause jamming of the flow of granular material, even under conditions where the cohesionless material flows. As cohesive forces become dominant large pores are formed in the bed, leading to substantial fluctuations in local (micro) density, and have been seen in powders leading to fluctuations in surface profiles, avalanche size and angle.[7,13,18] In recent years, researchers have attempted to quantify cohesion and flow characteristics of granular materials by primarily analyzing powder behavior in its consolidated state.[19-22]

Dilation is an important phenomenon in fine powder flow dynamics. Once any granular assembly is perturbed, it has to dilate (expand in volume) in order for flow to commence. As mixing dynamics depend on vessel fill levels in confined vessels (tumbling blenders), the amount of dilation can have a dramatic impact on the performance of blending processes. While it is known that density of cohesive materials varies substantially depending on shear history, flow-induced dilation has not been studied. The concept is not new; some early investigations of granular materials conducted by Hagen[23], and by Reynolds[24], formulated the idea of dilatancy (expansion of a closely packed assemblage of particles when the bulk is deformed). Endersby[25] found that loosely packed sands failed gradually, whereas tightly packed material failed by shear. However, very little fundamental understanding of the dilation phenomena exists today.

In the literature, most previous work on powder dilation is based on two-phase effects, where the presence of air either drives the flow (fluidized bed), or air needs to be displaced for the powder to flow (hoppers). In a fluidized bed, an increase in gas velocity increases the voidage to maximum (unlocking of the bed), resulting in a pressure drop equivalent to the weight of the bed[26]. Once the bed expands, the pressure drop remains constant and is not affected by increasing gas velocity. In the case of fine powders in hopper flow, pressure gradients in the interstitial gases lead to compression in the upper part of the hopper, and dilation in the lower part. [27-32]

A dense granular material resists shearing, both because of internal friction and because it must dilate to deform. The dilation of the bed weakens the interlocking between the particles and reduces the internal friction. However, cohesive forces increase normal stress at contact points between particles. According to Jaeger, dilation remains constant as no material can dilate infinitely and the state of deformation reaches steady state. For shear-induced dilation (as seen in tumbling blenders), it is unclear how important a role air entrainment plays in affecting the dynamics of dilation. Recently, Castellanos et al.[33,34] assigned air entrainment an important role in the mechanics of avalanche flow. They stressed that powders exhibit plastic flow properties and undergo a transition from the solid-plastic regime to the fluidized regime inside a rotating cylinder due to strong interaction between particles and interstitial air. However, the dynamics of dilation was not a focus of their study.

This article is organized into five sections. The first section describes the experimental setup and details of the experiments, the second section describes the simulation method and the model systems along with parameters used in this work. The quantification technique used for dynamic dilation is described in the third section. Simulation and experimental results and their interpretations are the subject of the fourth section. In this section, the main result is to demonstrate that dilation can be predicted using a model where air entrainment is not accounted for, providing a strong hypothesis that air is not a significant requirement for powders to dilate. The final section highlights the main conclusions of this work.

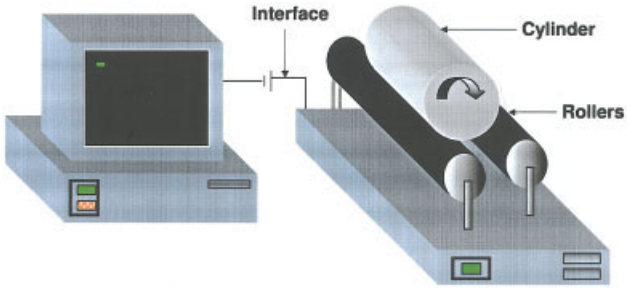


**Figure 1. Experimental setup.**

Cylinder setup on the roller, connected to a motor, interfaced to a PC. [Color figure can be viewed in the online issue, which is available at www.interscience.wiley.com.]

## Experimental Method

The experimental equipment used in this article, illustrated in Figure 1, is a computer-controlled roller assembly on which a cylinder up to 10 in. in dia. and 12 in. long can be mounted. The cylinders are made of transparent Plexiglas, which allows for observation of the flow dynamics and measurement of dilation of the powder within the cylinder. Digital video is set to capture images at the rate of 30 frames per s. In each experiment, the cylinder is loaded with the powder to 50% fill by volume. Experiments consider three rotation rates (7, 16 and 29 rpm) chosen to cover different powder-flow behavior. Data is recorded over the first 11 revolutions, during which the system reaches steady-state flow. The initial state of the powder is taken into account by pretreating the different powders in a similar way. This is done by shaking the powder bed horizontally and vertically a fixed number of times, and allowing the powder bed to settle by itself to maintain consistency in their initial states. The shaking also eliminates air entrainment that might have been caused during filling of the blender. External variables, such as humidity and temperature are kept the same.

An experimental device called the gravitational displacement rheometer has been developed for characterizing the cohesion of dry materials.[36] The flow indices, measured using the GDR, which is a measure of the cohesiveness of the powders are incorporated in Table 1.

*Materials.* We used suitable combinations of commercially available powders (Table 1) to create a family of "standard" systems of varying cohesion. Typical pharmaceutical excipients, glass beads and sugar were used, pure and in mixtures. These particles range from 50 $\mu$m to a few mm in dia. [Glass beads (noncohesive, 700 $\mu$m), fast-flo lactose (the least cohesive, 100 $\mu$m), Avicel 102 (90 $\mu$m), Avicel 101 (60 $\mu$m), Regular Lactose (50 $\mu$m, the most cohesive)]. These materials are some of the most common pharmaceutical excipients and in the interest of brevity their SEM images are not included in this article but can be found in multiple sources (see, for example, "*Handbook of Pharmaceutical Excipients*").[35]

**Table 1. Materials Used with Corresponding Size and Degree of Cohesiveness**

| Name | Size and Morphology | Flow Index | Vender, City, State |
|---|---|---|---|
| Glass bead | ~700 $\mu$m, sphere | 7.1 | Potter Industries, Carlstadt, NJ |
| Fast-Flo Lactose | ~100 $\mu$m, spherical | 27.8 | Foremost farms, Newark, NJ |
| Avicel 102 | ~90 $\mu$m, needle-like | 38 | FMC, Rothschild, WI |
| Avicel 101 | ~60 $\mu$m, needle-like | 44.2 | FMC, Rothschild, WI |
| Milled Lactose | ~50 $\mu$m, irregular shape | 48.0 | Foremost farms, Newark, NJ |

## Simulation Method

There are numerous models in the literature that deal with modeling cohesion using liquid bridge models.[37-39] The discrete element method (DEM), originally developed by Cundall and Strack,[40, 41] is used to simulate the dynamic behavior of cohesive powder in the rotating vessel. We considered frictional, slightly elastic particles, each of which may interact with its neighbors, or with the boundary only at contact points through normal and tangential forces. The normal forces (Eq. 1) between pair of particles in contact are calculated using the Walton and Braun's latching spring model[42, 43]

$$F_N = \begin{cases} K_1 a_1, & \text{for loading} \\ K_2(a_1 - a_0), & \text{for unloading} \end{cases} \quad (1)$$

The stiffness coefficients ($K_1$ and $K_2$) are chosen to be large enough to ensure that the overlap ($\alpha_0$ and $\alpha_1$) remains small compared to the particles sizes. Inelasticity of collisions is incorporated in this model by including a coefficient of restitution $e = \sqrt{K_1/K_2}$ ($0 < e < 1$, where $e=1$ implies perfectly elastic collision with no-energy dissipation, $e=0$ implies completely inelastic collision).

Tangential forces are calculated employing Walton's incrementally slipping model.[44] After contact occurs, tangential forces buildup nonlinearly, causing displacement in the tangential plane of contact. These forces obey Coulomb's law; if the magnitude is greater than the product of the normal force, and the coefficient of static friction, they lead to sliding with a constant coefficient of dynamic friction

$$\text{Sliding if: } F_T \geq \mu F_N \quad (2)$$

For simplicity, in this article, the static and dynamic-friction coefficients were considered of equal value in the simulations (future work will consider different values for dynamic and static friction). A list of the system parameters used in the simulations is given in Table 2.

In general, cohesion in particulate solids can be classified in two very broad types: "wet" and "dry" cohesion. In wet (or moisture-induced cohesion), capillary forces play a major role. In "dry cohesion", for solids smaller than 100 microns, Van der Waals forces become relevant, such as those calculated in the classical work by Johnson, et al. [45] and Derjaguin et al.[46] using contact mechanics. Electrostatic forces also become relevant for dry cohesion, affecting the flow of systems with particle size from one micron to a few mm. In this work, dry cohesive forces between two particles and between a particle, and the wall are simulated using a square-well potential, whenever particles are in contact. In order to compare simulations considering different number of particles, the magnitude of the force is represented by using the dimensionless parameter $K = F_c/mg$, where K is called the granular Bond number and is a measure of cohesiveness that is independent of particle size. This force is only added when there is particle/particle or particle/wall contact. The magnitude of the cohesive bond number K is not set arbitrarily. In fact, we chose a similar range for the values of K chosen by Baxter[47], which is supported by previous work by our group using AFM.[48]

The total resultant force on each particle is given by the sum of all the contact forces, gravitational force, and the cohesive force. The resultant torque is the sum of the moments of all the tangential contact forces acting on the particle. The procedure followed for simulations is similar to the experiments; initializing was carried out by vibrating the bed and then allowing it to settle under the influence of gravity.

### *Dilation measurements technique*

In this section we describe the details of the quantification technique used to measure dilation of the powder bed under confined conditions. Each of the experimental video images and numerical simulation snapshots are manually edited to further highlight the voidage fraction in the cylinder. Figure 2 depicts the quantification technique, where the granular bed is colored black and the voidage region is blue. A custom — designed pixel-counting program is used to determine the relative volumes of powder to void. It is assumed that bed dilation is uniform along the axis of the cylinder; visual observations and snapshots along the length of the cylinder support this assumption. Analysis of pixel data is done for snapshots taken at every 0.3 s for simulations and 1 s for experiments. The initial volume of the bed at time t = 0 s (no rotation) is considered as $Volume_{initial}$, and at any later time as $Volume_{new}$. Dilation is quantified as the percent increase in bed volume relative to the initial volume. Time t = 0 is taken as the last frame before the onset of powder movement

**Table 2. Parameters Employed in DEM Simulations**

| | |
|---|---|
| Total number of particles | 20,000 |
| Radius of the particles | 1.0 mm |
| Density of the particles | 1500 kg/m$^3$ |
| Frictional Coefficients | |
| Particle/particle | 0.4 |
| Particle/wall | 0.7 |
| Coefficient of restitution | |
| Particle/particle | 0.7 |
| Particle/wall | 0.5 |
| Normal Stiffness Coefficient | |
| Particle/particle | 6000 N/m |
| Particle/wall | 6000 N/m |
| Tangential Stiffness Coefficient | |
| Particle/particle | 4200 N/m |
| Particle/wall | 4200 N/m |
| Time step ($\Delta$t) | $2.5 \times 10^{-6}$ sec |

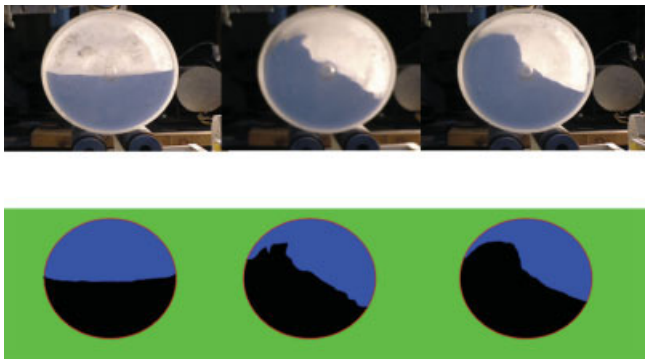

**Figure 2. Results from transforming the experimental pictures — the powder region is black, the voidage is blue, and the background is green.**

$$\% \text{ Increase in Bed Volume} = \frac{Volume_{new} - Volume_{initial}}{Volume_{initial}}$$

In order to evaluate the reproducibility of the experiments and the technique, multiple sets of experiments were carried out. As shown in Figure 3, for Avicel 101, the bed expansion was reproducible to within 5% RSD. Similar reproducibility was achieved for different materials, at different rotation rate and scale, which will be discussed in the next sections.

## Results

As will be discussed in the next sections, the aim of this article is to illustrate that the changes in packing, driven directly by cohesion, is a major factor in dilation. The fact that air is not accounted for in the simulations is a strong indicator that air entrainment is not the root cause for powders to dilate. This analogy contradicts Jaeger (who implies that dilation should be constant) and Castellanos (who emphasizes the role of air).

### *Mechanics of dilation*

Once a material has failed either through tensile cracking or by sliding, it flows down the surface of the cascade. Powder cohesion plays a strong role in determining the type/size of avalanches/failures and the flow dynamics. For completely free-flowing materials (that is, dry glass beads $\sim$200 $\mu$ or larger) run at moderate rotation rates (<30rpm), flow is continuous on the surface, and the flowing surface remains nearly flat. Particles flow as individual grains, enter the cascade, flow downward, and then re-enter the area of solid-body rotation. Dilation is minimal (< 5%); just enough to allow flow (similar to that described by Jaegar).

For slightly cohesive materials (fast-flow lactose), particles flow freely, resulting in nearly continuous flow in the form of waves (that is, weak avalanches). The free surface remains nearly flat, nearly smooth. As cohesion increases; in this case for Avicel 102, Avicel 101 and regular lactose, flow is characterized by distinct avalanches. Large portions of the material fail and flow down the surface in large avalanches. The size of avalanches is determined by the cohesive forces, and static friction between particles, while the speed of the avalanche is controlled by dynamic friction at the shear plane. We propose that an increase in cohesion plays a key factor in increasing dilation by increasing the porosity of the bed.

At a given shear rate, for free flowing material, the solid particles, which can flow freely, slide over each other providing a slight increase in the bed volume. As the cohesive forces between the particles increase, soft agglomerates (association of multiple particles) are formed, which similar to individual particles roll over each other under the effect of shear. In comparison to the free flowing case, the interstitial volume between the agglomerates is much larger, explaining the increase in bed porosity. The effect of rotation rate is insignificant (shown in next section), suggests that dilation is heavily dependant on cohesive forces. As cohesion increases, the shear applied is insufficient to break the cohesive forces causing increase in porosity and dilation.

### *Effects of cohesion*

Changes in powder dilation for the four pharmaceutical materials from Table 1, run at 7 rpm in the 8 in. dia. cylinder, are shown in Figure 4a. In general, dilation increased with increasing cohesion. The four powders show a similar trend, a radical increase in dilation (0 – 2 revolutions) occurs initially before settling to a steady-state regime. The least cohesive powder (fast-flo lactose) reaches steady-state almost immediately (<1 revolution). The more cohesive powders show more variability over the first few revolutions (especially regular lactose and Avicel PH102). The behavior for the first few revolutions is highly dependent on the initial conditions (packing fraction, length of time at rest, relative humidity, and so on). At steady state, the dynamic density of the materials was lower than the bulk density, indicating that dynamic dilation is much higher than static dilation. As seen in Figure 5, as particle cohesion increases, the difference between bulk density and dynamic density increased. It is not shown in this article that the degree of dilation did not vary significantly throughout the cylinder.

The degree of dilation was compared to the flow Index obtained from the GDR of the four materials and its mixtures. Here, mix 1 is a combination of 50% Fast-Flo Lactose and 50% Avicel 102; mix 2, that of Avicel 102 and regular lactose; and

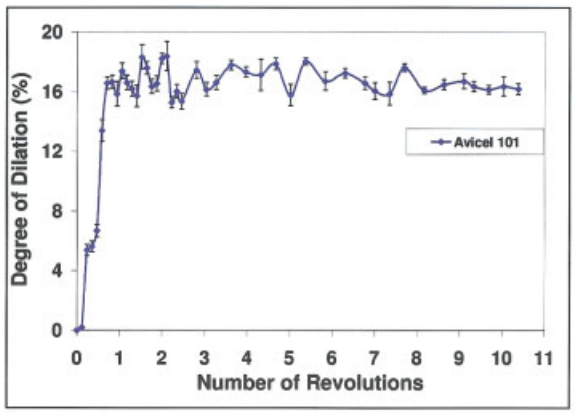


**Figure 3. Results for multiple runs on Avicel 101 shows the reproducibility of the methodology.**

[Color figure can be viewed in the online issue, which is available at www.interscience.wiley.com.]

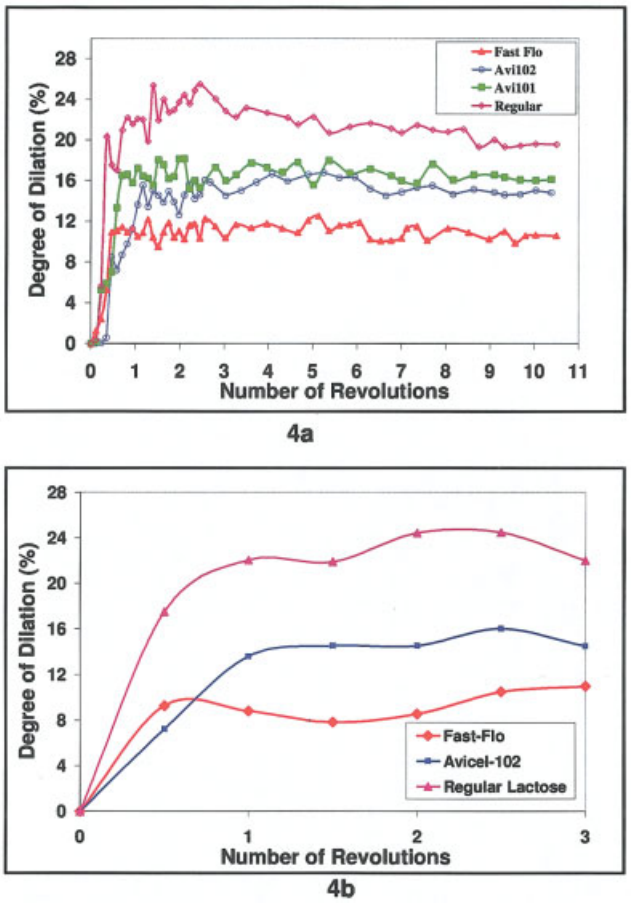


**Figure 4. (a) Plot illustrating the increase in dilation with powder cohesion for experiments, and (b) plot illustrating the increase in dilation with powder cohesion (increasing value of K) for simulations.**

[Color figure can be viewed in the online issue, which is available at www.interscience.wiley.com.]

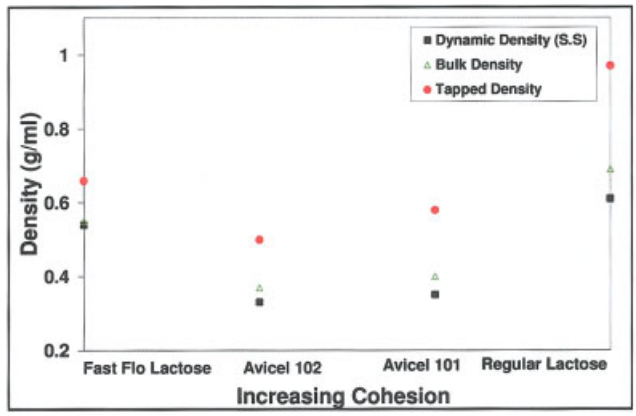


**Figure 5. Comparison of the dynamic density to the bulk and tapped density as a function of increasing cohesion in experiments.**

As powder cohesion increases, the difference in the dynamic and bulk density increases. [Color figure can be viewed in the online issue, which is available at www.interscience.wiley.com.]

### *Effect of the initial deformation of the powder on dilation*

As seen in Figure 4a, the maximum increase in bed expansion occurs in the first few revolutions. As the cylinder starts to rotate, static friction dominates the flow. A radical jump in dilation (0 – 2 revolutions) is observed during the initial deformation of the powder bed, which exhibits a tensile — cracking phenomena of larger intensity for powders of increasing cohesion. This initial deformation of the powder is mainly controlled by the relative strengths of static friction and cohesive bonding between the particles.

For the least cohesive powder, fast-flo lactose, the first major failure (white circle) is a weak avalanche (Figure 7a). For this weakly cohesive material, the only difference between the initial failures and the steady-state dynamics is simply a change in size and tempo. For Avicel PH102, the first major failure of mix 3 of Avicel 101 and regular lactose. As seen in Figure 6, there is an excellent correlation between the flow index and the degree of dilation. The bed expansion is a direct consequence of the cohesiveness of the powders and can also be used to quantify cohesion.

Experimental results of dilation are compared to those of simulation in Figure 4b. The simulation model shows the same trends as the experiments: dilation increases as K (that is, dimensionless cohesion) increases. The simulations show strong time-dependent initial behavior although the time scale over which steady state is reached is much shorter. The simulations are in qualitative agreement with experiments, despite the fact they neglect the effect of interstitial air. There is a difference in the quantitative values of simulations and experiments, due to the cylinder/particle size ratio for simulations being higher than for experiments, the fact that simulated particles are monosized and spherical. However, the clear implication appears to be that for cohesive materials at low-speed, air entrainment is a consequence, not a root cause of dilation.

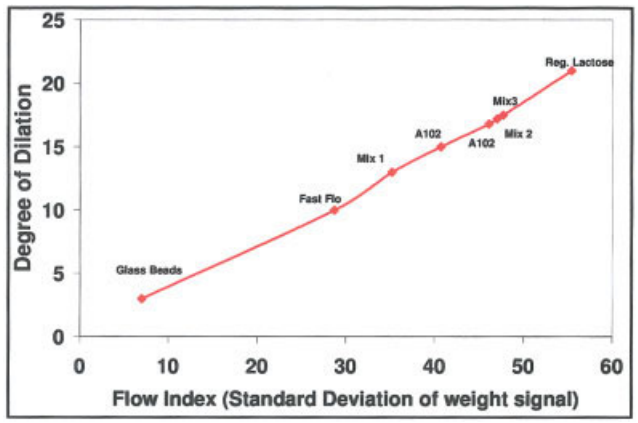


**Figure 6. Correlation of the flow index obtained from the GDR to the degree of dilation of the pure components and mixture blends.**

[Color figure can be viewed in the online issue, which is available at www.interscience.wiley.com.]

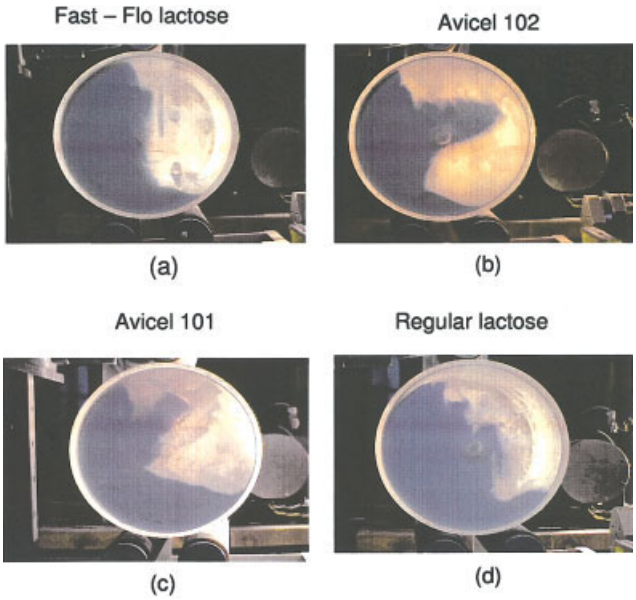


**Figure 7. Snapshot of the failure of the four pharmaceutical materials.**

As cohesion increases, the size of the failures (avalanches) increases. [Color figure can be viewed in the online issue, which is available at www.interscience.wiley.com.]

the material occurred when a large portion of material broke off through a tensile-cracking mechanism (Figure 7b). The next few failures were similar in nature although smaller and only after the entire powder bed had circulated through the flowing region at least once did the dynamics approach the frictionally-controlled steady-state.

The more cohesive Avicel PH101 did not exhibit any initial small avalanches before the onset of major bulk failure. The free surface of the material had to travel almost to a 90-degree angle until any relative motion in the powder bed was noted. The first evidence of movement occurred at the "top" of the cylinder where the powder broke free from the cylinder wall (Figure 7c). The first failure was similar to Avicel PH102; a large portion broke off through tensile failure and crashed downward. The next few failures were similar in nature, but smaller in size until the steady-state friction-controlled dynamics were reached.

Finally, Regular lactose separated from the wall much sooner that any of the other materials, indicating that the bond between particles and wall was weakest for this material (relative to material density). After separating from the wall, a large portion of the material near the free surface appeared to break away from the bulk and slide downward (Figure 7d). The topmost section exhibited tensile cracking, but the entire ensemble flowed down the cascade rather than breaking off and cracking like the Avicels. Further failures were very similar, although it took the longest for this material to approach steady-state.

### *Air, dilation, and coordination number*

In the case of fine powders, the attractive forces between particles can lead to agglomeration: bridging, coating and buildup. These forces are short range and typically weak, leading to formation of soft agglomerates. The intensity of particle adhesion increases as the cohesive stresses increases (finer particles), leading to bigger aggregates. This suggests that the variation of the bed porosity is mainly controlled by the cohesive forces. As shear is insufficient to overcome the effect of cohesive forces, and breakup these agglomerates, the formation of larger agglomerates allows for larger pore size distribution in the bed causing higher dilation.

One method to examine this phenomenon is by analyzing the coordination number of the particles in the simulations. We estimated the particle coordination number distribution for varying levels of cohesion. Figure 8 shows the variation of the mode of distribution as a function of cohesion factor "K" at time $t = 4$ s, when the bed has already been dilated. Increase in cohesion "K" results in lowering of the coordination number once flow has been induced.

### *Effects of speed*

Figure 9 shows the effect of rotation rate on dilation of the powders studied here. For the least cohesive powder, fast-flo lactose, dilation increases with increases in rotation rate (Figure 9a). In a rotating cylinder, this material exhibits nearly continuous flow on the surface and rather than observing individual avalanches, the cascading surface undulates aperiodically. Avalanches are neither discrete nor separated. As the rotation rate increases, the particles on the surface increase in velocity, which may imply a shallower flowing layer. It is likely that the increase in dilation is asymptotic and that above a certain rotation rate, dilation will no longer increase. Furthermore, at higher-rotation rates, the material becomes airborne at the top of the flowing layer and measuring dilation becomes haphazard at best. Figures 9b and c show the dilation of higher-cohesion powders (Avicel PH-101, Regular Lactose). For these materials, increases in rotation rate do not lead to steady-state increases in the degree of dilation. It is surmised that the faster rotation rates leads to an increase in the frequency of avalanches without significantly changing the dynamics of flow, thereby not causing change in dilation. Simu-

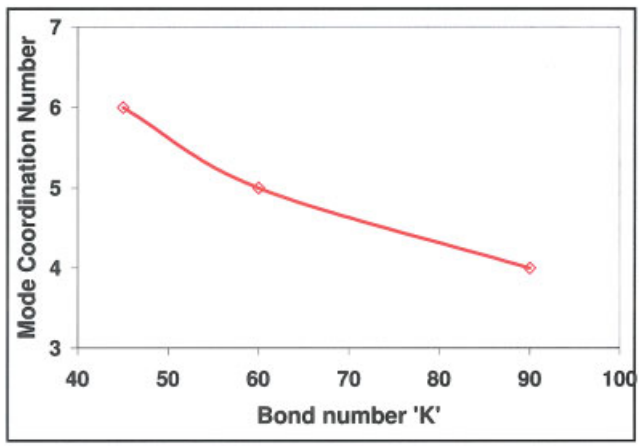


**Figure 8. Plot of Coordination Number vs. Granular bond number using DEM simulations.**

When flow is induced, coordination number decreases as "K" increases. [Color figure can be viewed in the online issue, which is available at www.interscience.wiley.com.]

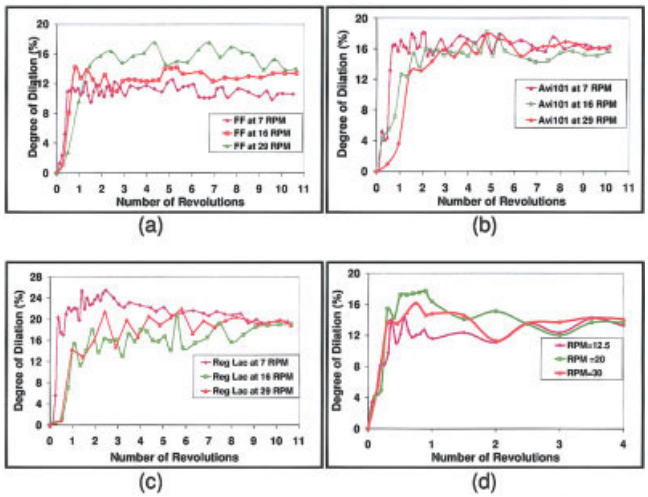


**Figure 9. Changes in dilation with increasing rotation rate are shown for (a) fast-flo lactose, (b) Avicel PH101, (c) regular lactose, and (d) simulations using K = 90 (most cohesive).**

While there is short-term variability in most cases, only fast-flo lactose (the least cohesive) material shows changes in steady-state dilation with change in rotation rate. [Color figure can be viewed in the online issue, which is available at www.interscience.wiley.com.]

lations were also performed at multiple rotation rates for K = 90 (high-cohesion), and the same trend was noted (Figure 9d). For both experiments and simulations, there is short-term variability in dilation but the steady-state value does not vary with increasing rotation rate. Perhaps, there exists a different regime at higher-rotation rate, which can be a cause for further investigation.

### *Effects of cylinder diameter*

Experiments investigating change in dilation with variations in cylinder diameter (1–10 in.) were performed with Avicel 101 because this material exhibited the widest range of avalanching behaviors. As the diameter of the container was increased from 1 to 8 in., dilation decreased monotonically due to an increase in shear, which causes the agglomerate to break up (Figure 10a). However, when the diameter was increased to 10 in., dilation suddenly increased to the highest value of all the experiments (this surprising result was reproduced numerous times). In the smallest cylinder, flow was constrained and periodic, and a relative large value for dilation was measured. The shear provided was insufficient to break the agglomerates. This is similar to the case of high-powder cohesion. As the cylinder diameter increased, flow became freer; particles were able to move as individual grains. In the 10 in. cylinder (excellent reproducibility was achieved), flow was free, but would stop before reaching the end wall of the cylinder, as the shear was insufficient to allow the material to cascade down the cylinder. The insufficient shear prevented the breakage of agglomerates, causing the degree of dilation to reach its maximum. We also carried out simulations for similar range of vessel diameter, and the results were comparable to that of the experiments as shown in Figure 10b.

Thus, it appears that dynamic friction (resistance to flow after the initial deformation/failure) imposes a length scale for the travel distance of the failure/avalanche. If the cylinder diameter is less than this travel distance, flow is restricted and dilation will increase as the diameter increases. The shear tends to get distributed through out the whole bed. At some optimum cylinder diameter, "free" flow will be maximized as the shear is distributed only at the top surface, thereby enabling dilation to reach a minimum. As the cylinder size is increased beyond this optimal size, the shear provided is insufficient to cause the agglomerates to break, thus, not allowing the particles to move freely.

In previous work with mixing of powders, a similar trend was noted — mixing rates decreased over a certain range of increasing blender volumes, but then increased dramatically for the largest blender. Thus, for both dilation and mixing rates, there was a range over which one trend was noted, and then above a certain size the trend completely reversed itself. Observation of the flow in the vessel indicated that flow dynamics (especially near the bottom of the cascade) appeared to play the

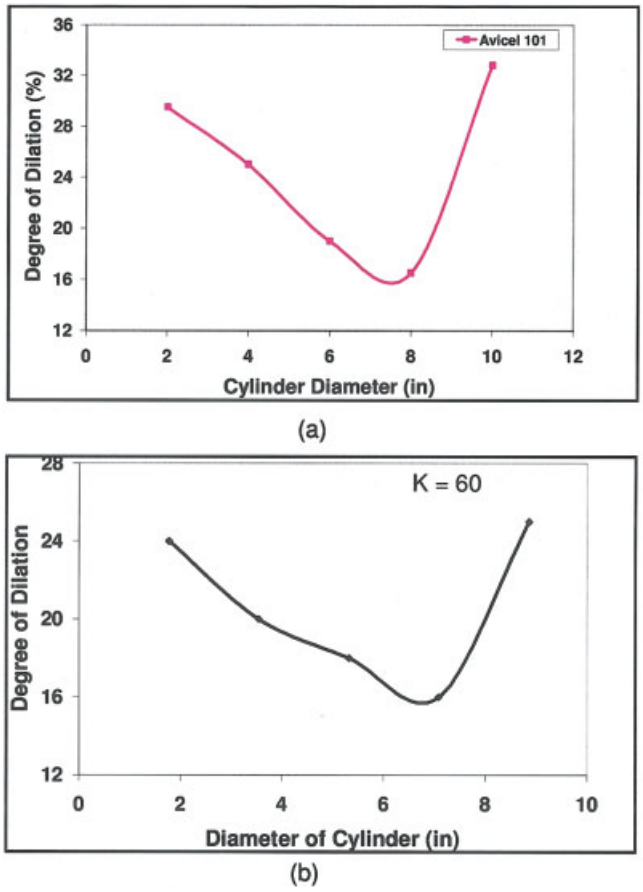


**Figure 10. (a) Change in dilation for Avicel PH101 is shown for cylinders ranging from 2 inch dia. to 10 inch dia.. Dilation decreases monotonically as cylinder dia. increases from 1–8 inches, but then rises dramatically in the 10 in. cylinder, and (b) shows the results of varying diameter for simulations (K = 60).**

[Color figure can be viewed in the online issue, which is available at www.interscience.wiley.com.]

major role in determining changes in dilation with increasing scale.

## Conclusions

In general, an increase in cohesion leads to an increase in dilation. The difference in the initial deformation was due to the static friction between the particles. The simulations were in excellent qualitative agreement with experiments, where increase in the cohesion factor "K", led to increase in dilation. The fact that air is not accounted for in the simulations is a strong indicator that air entrainment is not a necessary dynamical ingredient for powders to dilate, and that alternative mechanism can play a dominant role. The effect of rotation rate was relevant for low cohesion; increasing the rotation rate increased dilation, but only slightly. The effect of scale is pivotal as dynamic friction seems to impose a length scale for the traveling distance of an avalanche.

We caution that this analysis has been verified for relatively short (12 in. length) cylinders of small diameter/capacity (1–10 inches), and it is unclear how changes in blender size, geometry, and surface properties will affect changes in dilation. It is apparent, however, that dilation is an important factor to consider when loading a tumbling blender. The total volume taken up by the material can change drastically between the resting state and steady-state in motion. Mixing failures could be caused by the ensuing "overfilling" of the blender caused by the dilation of the powder beyond the limits of useful blender operational range. As the particle cohesion increases, flow dynamics change from a regime where motion of individual grains dominate to that controlled by motion of agglomerates formed due to cohesive forces. The increase in cohesion not only affects the flow dynamics, but it also changes the structure of the granular bed. In particular, it was found that due to the domination of cohesive forces over shear forces, the porosity of the bed could be considerably increased. Such large variations in bed porosity can have tremendous consequences for product uniformity and quality, since regions of high and low solid densities can coexist within a blender.

## Literature Cited


1. Bagnold RA. *The physics of blown sand and desert dunes.* London: Chapman and Hall; 1941.
2. Bagnold RA. Experiments on a gravity-free dispersion of large solid spheres in a Newtonian fluid under shear. *Proc R Soc Lond*. 1954; A225:49-63.
3. Savage SB, Tuzun U, Houlsby GT, Nedderman RM. The flow of granular materials - III Rapid shear flows. *Chem Eng Sci*. 1983;38: 189-195.
4. Savage SB. The mechanics of rapid granular flows. *Adv Appl Mech*. 1984; 24:289 -298.
5. Savage SB, Hutter K. The motion of a finite mass of granular material down a rough inclined plane. *J Fluid Mech*. 1989;199:177-215.
6. Wightman C, Mort PR, Muzzio FJ, Riman RE, Gleason RK. The structure of mixtures of particles generated by time-dependent flows. *Powder Technol*. 1995;84:231-240.
7. Metcalfe G, Shinbrot T, McCarthy JJ, Ottino JM. Avalanche mixing of granular materials. *Nature*. 1995;374:39-41.
8. Pierrat P, Caram HS. Tensile strength of wet granular materials. *Powder Technol*. 1997;91:83-93.
9. Mikami T, Kamiya H, Horio M. Numerical simulation of cohesive powder behavior in a fluidized bed. *Chem Eng Sci*. 1998;53:1927-1940.
10. Adams MJ, Perchard V. The cohesive forces between particles with interstitial fluid. Inst. *Chem Eng Symp*. 1985;91:147-160.
11. Lian G, Thornton C, Adams MJ. A theoretical study of liquid bridge forces between two rigid spherical bodies. *J Colloid Interface Sci*. 1993;161:138-147.
12. Bocquet L, C.E., Ciliberto S, Crassous J. Moisture-induced ageing in granular media and the kinetics of capillary condensation. *Nature*. 1998;396:735-737.
13. McCarthy JJ, Nase S, Vargas WL, Abatan AA. Discrete characterization tools for cohesive granular material. *Powder Technol*. 2001;116: 214-223.
14. Moser S, Sommer K. Calculation of van der Waals forces in adhering systems. *Powder Technol*. 1977;17:191-195.
15. Stotzel H, Schmidt HJ, Auerbach D, Makin D, Dasttoori BK, Bauch H. Adhesion measurements for electrostatic powder coating. *J of Electrostatics*. 1997;40:253-258.
16. Feng JQ, Hays DA. Relative importance of electrostatic forces on powder particles. *Powder Technol*. 2003;135:65-75.
17. Yang Y, Sliva A, Banerjee A, Dave RN, Pfeffer R. Dry particle coating for improving the flowability of cohesive powders. *Powder Technol*. 2005;21-33.
18. Lim SY, Davidson JF, Forster RN, Parker DJ, Scott DM, Seville JPK. Avalanching granular material in a horizontal slowly rotating cylinder: PEPT studies. *Powder Technol*. 2003;138:25-30.
19. Johanson JR. Johanson indicizer system vs. the Jenike shear tester. *Bulk Solids Handling*. 1992;12:237- 240.
20. Carr RL. Evaluating flow properties of solids. *Chem Eng*. 1965;72: 69-72.
21. Doung NH, Shen E, Shinbrot T, Muzzio FJ. Segregation in granular materials and the direct measurement of surface forces using atomic force microscopy. *Powder Technol*. 2004;145:69-72.
22. Orband JLR, Geldart D. Direct measure of powder cohesion using a torsional device. *Powder Technol*. 1997;92:25-33.
23. Hagen G. Druck und bewegung des trockenen sandes. *Berl Monatsb Akad d Wiss*. 1852;35-42.
24. Reynolds O. On the dilatancy of media composed of rigid particles in contact. *Philos Mag Ser*. 1885;20:469-481.
25. Endersby VA. The mechanics of granular and granular-plastic materials, with special reference to bituminous road materials and subsoils. *A Soc Text Mater*. 1940;40:1154-1173.
26. Leva M. *Fluidization*. New York: McGraw-Hill; 1959.
27. Meyers ME, Sellers M. *Tripos Project Report*. University of Cambridge Department of Chemical Engineering: London; 1978
28. Nedderman RM, Tuzun U, Savage SB, Houlsby GT. The flow of granular materials - discharge rate from hoppers. *Chem Eng Sci*. 1982;37:1597-1609.
29. Nedderman RM. *Statics and Kinematics of granular materials*. 1st ed. Cambridge University Press; 1992:352
30. Ouwerkerk CED, Molenaar HJ, Frank MJW. Aerated bunker discharge of fine dilating powders. *Powder Technol.* 1992;72(3): 241-253.
31. Crewdson BJ, Ormond AL, Nedderman RM. Air-impeded discharge of fine particles from a hopper. *Powder Technol*. 1977;16:197-207.
32. Beverloo WA, Leniger HA, Velde JVD. The flow of granular solids through orifices. *Chem Eng Sci*. 1961;15:260-269.
33. Castellanos A, Valverde JM, Quintanilla MAS. Fine cohesive powders in rotating drums: Transition from rigid-plastic flow to gas-fluidized regime. *Phys Rev E*. 2002;65:61301.
34. Castellanos A, Valverde JM, Perez AT, Ramos A, Watson PK. Flow regimes in fine cohesive powders. *Phys Rev Lett*. 1999;82:1156-1159.
35. Rowe R, Sheskey P, Weller P. *Handbook of Pharmaceutical Excipients.* 4th ed. New York, APhA Publications; 2003.
36. Chaudhuri B, Alexander A, Faqih A, Muzzio F, Tomassone M. Avalanching flow of cohesive powders. *Powder Technol*. 2006;164:13–21.
37. Thornton C, Ning Z, A theoretical model for the stick/bounce behavior of adhesive, elastic-plastic spheres. Powder Technol. 1998;99:154-162.
38. Lian G, Thornton C, Adams MJ. Discrete particle simulation of agglomerate impact coalescence. Chem Eng Sci. 1998;53:3381-3391.
39. Thornton C, Ciomocos MT, Adams MJ. Numerical simulations of diametrical compression tests on agglomerates. *Powder Technol*. 2004; 140:258-267.
40. Strack ODL, Cundall PA. A Discrete numerical model for granular assemblies. *Geotechnique*. 1979;29:47-65.
41. Cundall PA. A computer model for simulating progressive large-scale

movements in blocky rock systems. *Proc Symp Int Soc Rock Mech*. 1971;2:129-136.
42. Walton OR. Numerical simulation of inelastic, frictional particle-particle interactions. *Particulate Two-Phase Flow*. 1992;16:884-911.
43. Walton OR. Numerical simulation of inclined chute flows of monodisperse, inelastic, frictional spheres. *Mechanics of Materials.* 1993; 16:239-247.
44. Walton OR, Braun RL. Viscosity, granular-temperature and stress calculations for shearing assemblies of inelastic, frictional disks. *J Rheol*. 1986;30:949-980.
45. Johnson KL, Kendall K, Roberts AD. Surface energy and the contact of elastic solids. *Proc R Soc Lond A*. 1971;324:301.
46. Derjaguin BV, Muller VM, Toporov YP. Effect of contact deformations on the adhesion of particles. *J Colloid Interface Sci*. 1975;53:314.
47. Baxter J, Abouchakra H, Tuzun U, Lamptey BM. A DEM simulation and experimental strategy for solving fine powder flow problems. *Trans IChemE*. 2000;78:1019-1025.
48. Duong N, Shen E. Shinbrot T, Muzzio FJ. Segregation in granular materials and the direct measurement of surface forces using atomic force microscopy. *Powder Tech*. 2004;145:69-72.

*Manuscript received June 9, 2005, and revision received Aug. 2, 2006.*